Operational Techniques for Determining SWE by Sound Propagation through Snow: II. Instrumentation and Testing

NICHOLAS J. KINAR[1] AND JOHN W. POMEROY[1]

ABSTRACT

To show that the acoustic technique of determining SWE can contribute to operational SWE surveys, portable, field-usable devices were constructed with the capability of reliable on-line signal processing and calculation of SWE in the field. The portable field devices were tested at forest and tundra sites near Whitehorse, Yukon Territory, and at forest and meadow sites in the Rocky Mountains, Alberta, Canada. Comparisons were made between the acoustic technique and gravimetric sampling, which was conducted using snowpits, density samples of individual snow layers and an ESC30 "snow tube" snow density sampler and ruler. These comparisons demonstrated that the acoustic measurement with the portable field unit and on-line modified signal processing technique can provide SWE estimates in the field that are of comparable accuracy to SWE calculated from gravimetric samples. The on-line processing allows the operator to gauge the reliability of the measurement and to ensure sufficient data collection before leaving the field site. Significant advantages over gravimetric sampling accrue from non-destructive sampling of the snowpack and ease of measurement. A sensitivity analysis of the acoustic model is presented. Limitations and aspects for further research are also discussed.

INTRODUCTION

In a previous paper (Kinar and Pomeroy, *this issue*) we discussed the operational theory of determining SWE by an acoustic wave. To provide an instrument capable of producing on-demand estimates of SWE from the theory, custom electronic circuits were made and tested. This paper describes the sampling system and the tests which were used to validate the acoustic sampling technique.

APPARATUS

Overview

Two portable prototype devices were constructed to implement the calculations of SWE. With the exception of a few minor changes, both systems had similar functionality.

The first system was only able to send the sound wave into the snowpack and record the reflected wave. Post-processing of the data was required to estimate SWE. Because the data collected by the instrument were not processed in the field, this allowed for the theory and signal processing to be tested before constructing a more finalized version of the circuit. The first system was initially designed to send and produce frequency-swept chirps. Field testing of the first system with frequency-swept chirps produced results that could not be fully automated. Numerical

[1] Centre for Hydrology, University of Saskatchewan, 117 Science Place, Saskatoon, Saskatchewan, S7N 5C8 Canada.

solutions of the first acoustic model (Kinar and Pomeroy, 2007) for the frequency-swept chirps were unstable, and could not be always performed by software in an autonomous fashion. The first prototype system was also used to produce short (~1 second) Maximum Length Sequences (MLS) after the frequency-swept chirps had been sent into the snowpack (Borish and Angell, 1983; Rife and Vanderkooy, 1989). MLS signals allowed for SWE to be calculated autonomously (Kinar and Pomeroy, 2008).

The second system was designed specifically to send MLS sequences from the loudspeaker. This system had the capabilities to perform signal processing on the data and to show the calculated values for SWE on an LCD display mounted in the circuit enclosure, allowing for an investigator to estimate SWE in the field without post-processing. An acoustic sampling event was initiated by a pushbutton switch mounted on a trigger grip fastened to the underside of the electronic circuit box. The peak detector which identified reflections from the snowpack used an estimate Y^* of the average snow depth (Kinar and Pomeroy, 2008). The keypad on the second system allowed for the user to enter an estimate of Y^* after measuring the snow depth with a snow depth ruler.

Measurement system

The system was created as a custom electronic circuit. Initial versions of some sub-circuits comprising the system were built on perforated construction boards and wires were joined by hand to create electrical connections. More permanent versions of each circuit were created in the form of printed circuit boards with surface-mount components. The circuit boards were mounted in enclosures which allowed the system to be transported to field locations. A block diagram of the system is given as Figure 1. Pictures of the two system prototypes are also given (Figure 2). The Analog-to-Digital converter (ADC) sampled the received signal at 96 kHz.

System parameters

Estimates of numerical values for the sound power P_0, aperture angle φ of the loudspeaker, and the microphone sensitivity L_s are required for the signal processing procedure (Kinar and Pomeroy, 2008), and to calculate the footprint of the beam on the snow interfaces (Kinar and Pomeroy, *this issue*). Prior to deployment of the circuits at the field sites, the sound power P_0 of the loudspeaker was determined as $P_0 = 9.2$ Watts by integrating the Root Mean-Square (RMS) pressure produced by the loudspeaker over the area of a parallelepiped. This procedure for determining the sound power of a source is similar to the procedures discussed in the ISO 3744 and ISO 3745 standards (Raichel, 2006). The aperture angle φ of the loudspeaker was determined as $\varphi = 10$ degrees by spatial measurements of sound intensity made with a microphone placed in the far field of the loudspeaker. The aperture angle was defined as the angle beyond which $I / I_0 \leq 0.1$, which represents a 10dB drop in sound intensity I from the axial intensity I_0 of the source (Kinsler and Frey, 1962). The electret microphone sensitivity of $L_s = -35$dB (with reference to 1 V per Pa) was estimated from the microphone's output voltage when the capsule was situated on-axis and in the far field of a 100dB SPL source. All of these measurements were made at room temperature (~20°C).

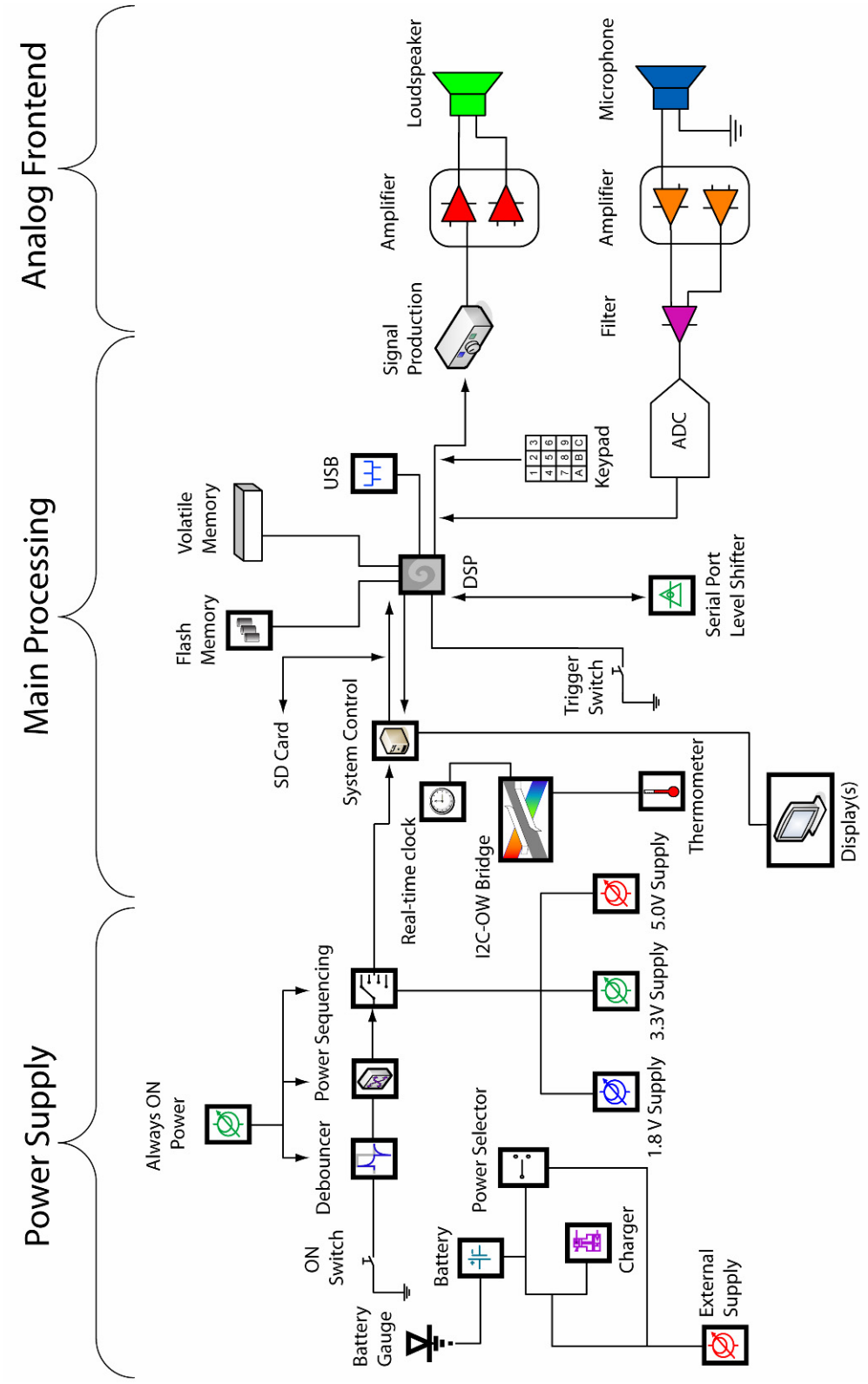

Figure 1. Block diagram of the system, showing the power supply, main processing, and analog frontend block

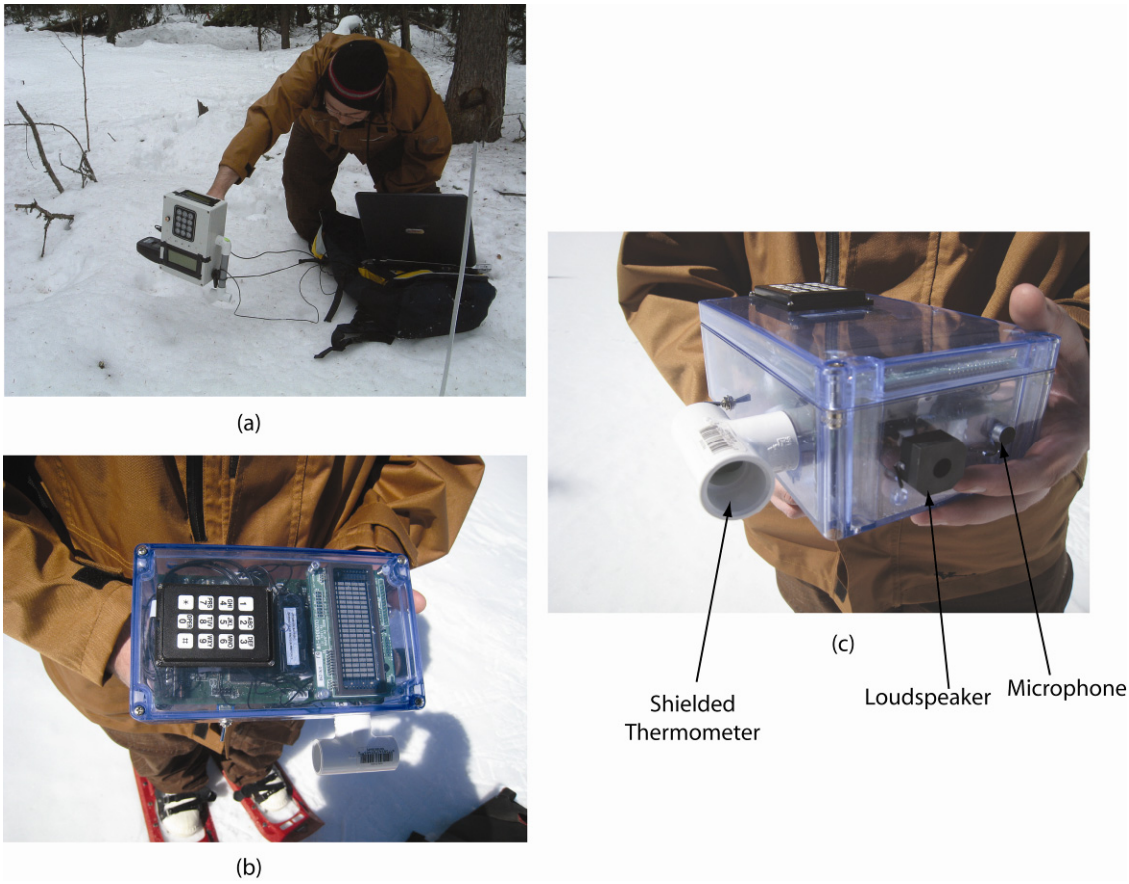

Figure 2. Pictures of the two prototype circuits. The first prototype is shown as (a), and the second prototype is shown as (b). A front view of the second prototype gauge showing the loudspeaker and the microphone is given as (c).

EXPERIMENTAL LOCATIONS

Wolf Creek, Yukon Territory

Wolf Creek Research Basin is a mountainous catchment located near Whitehorse, Yukon. Vegetation cover is primarily shrub tundra, alpine tundra and boreal forest (Granger, 1999). The first prototype of the acoustic gauge was tested during April 2007 in the valley bottom of Granger Basin (GB), a sub-catchment situated within the Wolf Creek Basin. The vegetation at this site was representative of shrub tundra composed of willow and birch from 30 cm to 2 m tall. Snow at GB was heavily crusted by wind and melt, but was cold and dry with extensive depth hoar formation. Additional tests were also conducted under the canopy of a discontinuous white spruce stand in the boreal forest (BF) at lower elevations in Wolf Creek Basin.

Rocky Mountains, Alberta

The second prototype of the acoustic gauge was tested during May 2008 in the Spray River valley east of Banff National Park. The first test site was situated less than one km from the Burstall Pass trail parking lot. Testing was conducted in an open area near a sub-alpine forest (BP-open) and on a ridge (BP-ridge) near the parking lot. BP-open snow was melting with air temperatures near 7° C during sampling. BP-ridge snow had undergone melt but was cold and relatively dry during sampling. The Mount Shark sampling locations (MS) were situated near the Mount Shark parking lot in an area interspersed with sparse fir (*Abies* sp.) and spruce (*Picea* sp.) trees. Snow here was similar to the BP-ridge snow.

PROCEDURE

Yukon sites

Eight sampling locations were selected along a transect in the valley bottom of Granger Basin (GB). At each sampling point, the first prototype device was pointed at the snow surface and an acoustic measurement of SWE was initiated by pressing the trigger button. After the acoustic SWE sample was collected, a snow pit was dug directly under the measurement point and SWE was determined by gravimetric sampling. Observations were also made of the presence of vegetation trapped beneath the snow surface. Many samples had willow shrubs buried under the measurement site. A hard wind crust was observed on the top of the snowpack, and ice layers were scattered throughout the snowpack.

This acoustic sampling technique was repeated under the boreal forest canopy (BF). Due to the presence of trapped vegetation and forest detritus beneath the snow surface, it was not possible to dig a snow pit at all of the sampling locations. Fourteen sampling locations were identified. An acoustic measurement of SWE was taken before disturbing the snow surface. At these locations, SWE was estimated using a snow pit and an ESC30 snow sampler.

Rocky Mountain sites

At the Burstall Pass test site (BP-open) before the snow surface was disrupted, the second prototype device was used to take samples at five points. Snow pits were then dug at each of the points, and gravimetric sampling was used to determine the SWE of each sample point. Gravimetric SWE measurements with an ESC30 snow sampler were also taken. Because the sampling procedure occurred during the morning and mid-afternoon, the snowpack was slightly wetted at the surface but generally dry at depth.

A second transect was set up along a ridge overlooking the Burstall Pass parking lot (BP-ridge). Acoustic sampling with the snow sonar device was conducted at 13 sampling points situated in the open and in close proximity to shallow snow near large coniferous trees. Immediately after using the acoustic SWE device, gravimetric samples of SWE were taken with an ESC30 snow sampler. Because the sampling occurred during the morning, the snowpack was refrozen and dry.

Sampling in the Mount Shark area occurred along a transect situated between the trees (MS). The acoustic gauge was used to sample in the vicinity of tree wells and in the open, unsheltered areas. Gravimetric measurements of SWE were taken with an ESC30 snow sampler at each of the acoustic sampling points. The snowpack was observed to be dry, and the snow surface was hard and icy. All measurements were completed before the surface of the snowpack started to become wet.

RESULTS AND ANALYSIS

Example calculation

To demonstrate the procedure used to determine SWE by acoustics, an example calculation was performed for a point at the GB site (Table 1). Figure 3 shows the signals involved in signal processing.

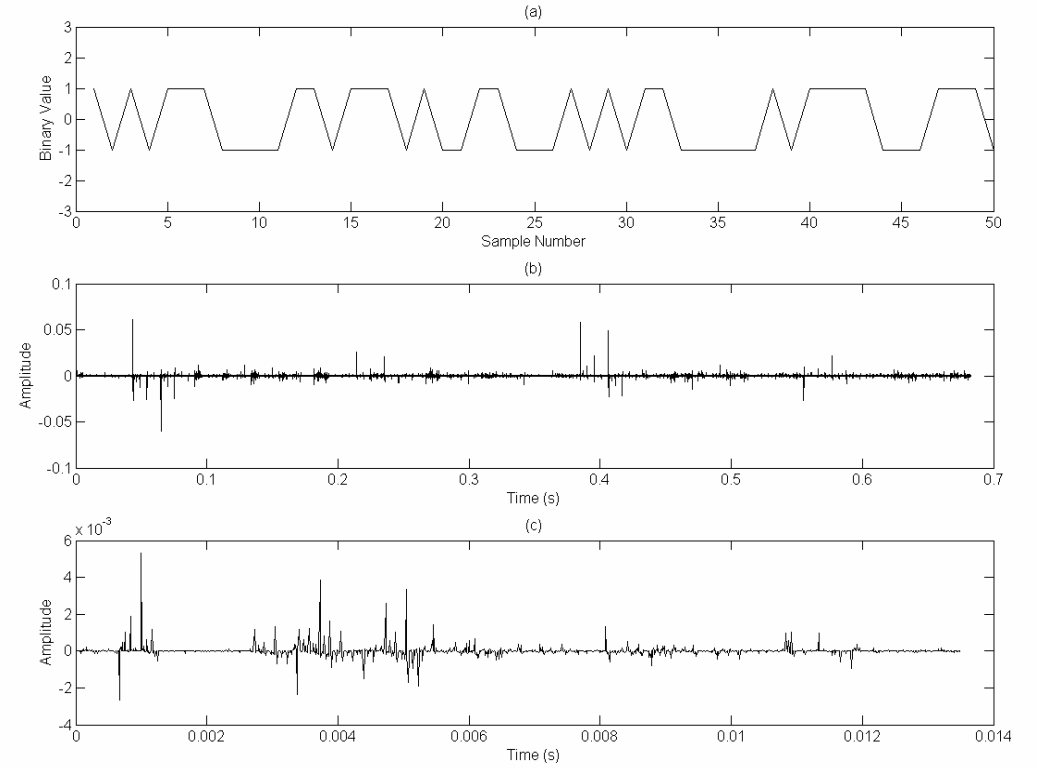

Figure 3. Signals sent and received by the acoustic gauge. Explanations of the figures are given in the text.

The signal sent from the loudspeaker was a Maximum Length Sequence (Figure 3a). The generation of the sequence is discussed by Kinar and Pomeroy (2008). The reflection response (Figure 3b) is calculated using the signal processing procedure described by Kinar and Pomeroy (2008). The reflection response truncated by the time taken for the sound wave to travel over the estimated snow depth Y^* is depicted as Figure 3c. The signal is truncated because peaks observed after the maximum two-way travel time are multiple reflections from the snowpack or from other objects (i.e. trees, the experimenter holding the device).

The truncated reflection response (Figure 3c) is comprised of "peaks" that were identified by an automated peak detector. Peaks are coincident with reflections of the sound wave by "layers" in the snowpack. The times at which each peak occurs is listed in Table 1. Further description of the peaks is given by Kinar and Pomeroy (2007).

The modeled acoustic snow depth of $Y = 0.8457$ m is close to the measured snow depth of 0.85 m. This is to be expected because the maximum cutoff time of the peak detector (Kinar and Pomeroy, 2008) has been calculated from the measured snow depth.

The average acoustic snow density for this sampling point was $\overline{\rho} = 396$ kg m^{-3}, and the measured gravimetric snow density was 370 kg m^{-3}. There is a 7% difference between the measured and modeled snow densities. The snow density determined by the acoustic technique was over-predicted by 26 kg m^{-3}. The density may have been over-predicted due to the changing phase velocity of the P_2-wave as it propagated through the porous snow medium, which occurred for frequencies lower than $\tilde{\omega}$. The acoustic SWE was found to be SWE = 335 mm. The acoustic SWE was calculated by multiplying the average of the snow densities of each layer by the average acoustically-determined depth. The SWE determined by depth measurements and gravimetric sampling was SWE = 315 mm. There was a 6% difference between the acoustic and gravimetric measurements of SWE. The acoustic measurement of SWE was over-predicted due to over-prediction of the density.

The average acoustic tortuosity of the sampling point was greater than unity ($\overline{\alpha} > 1.0$), which suggests that the pore space geometry has a complex and twisted structure that cannot be exactly

modeled as $\overline{\alpha} = 1.0$. Because measurements of tortuosity were not determined by another method, it is impossible to make quantitative comparisons between acoustic and measured properties.

The calculated attenuation (Kinar and Pomeroy, 2008) of the P_2-wave in the pore spaces of the snowpack suggests that snow strongly attenuates sound. Sound Pressure Level (SPL) is a measurement of the Root Mean-Square (RMS) pressure of the sound wave, relative to the smallest pressure that can be heard by a human being. It is widely used in sonar engineering to characterize the reduction of sound pressure at a distance away from a source. The average reduction in Sound Pressure Level of the sound pressure wave as it propagated was approximately 94 dB. This measurement of attenuation is within the order of magnitude of attenuation measurements made from microphones buried within the snowpack (Moore *et al.*, 1991), and helps to support the conclusion (Albert, 1993) that snow is a highly dispersive medium. However, because the attenuation value is the average attenuation for the MLS signal sent into the porous snow medium, it is possible that this value is over-predicted due to the attenuation of the higher frequencies in the signal. Independent measurements of the frequency-dependent attenuation of snow are required to properly compare these attenuation values.

Table 1. Acoustic model output.

Time at Peak (s) t_k	Snow Density (kg m^{-3}) ρ_k	Layer Thickness (m) y_k	Layer Tortuosity α_k	Attenuation Coefficient (m^{-1})	Attenuation[a] (SPL dB) $8.69\psi_k y_k$
0.0010	68.6681	0.1648	1.0478	0	0
0.0034	174.3421	0.3831	1.1385	25.7342	85.5661
0.0047	473.2300	0.2084	1.6292	53.4851	96.7708
0.0050	572.3230	0.0403	1.9797	281.8227	98.5128
0.0055	690.6107	0.0489	2.7998	232.3792	98.7238
Average	**395.8348**	**0.1691**	**1.7190**	**148.3553**	**94.8934**

[a]The average of the attenuation values does not include the first air layer above the snow surface, which has negligible attenuation.

These measurements of attenuation may represent the first time that the attenuation of sound in snow has been measured in a non-invasive fashion with an MLS sequence. As recognized by (Albert, 1993), disrupting the snowpack may modify the snow structure, and consequently change the acoustic properties of the snowpack. Non-invasive measurements allows for the attenuation to be determined without modification of the snowpack structure.

Yukon sites

Results from the Granger Basin site (GB, Figure 4, Table 2) demonstrate the effects of vegetation and even snowpack layering on the acoustic technique. The presence of a hard wind crust (sample point 2) was observed to have a small effect on the acoustically-determined SWE. Sample point 3 demonstrated the effects of a buried shrub on the output of the acoustic device. The acoustic SWE was over-predicted due to scattering of the sound wave by the buried vegetation. Because the acoustic density was under-predicted at this point, the acoustic depth was over-predicted due to multiple returns from the buried vegetation. In contrast to sample points 6 and 7, which are characterized by low vegetation heights, the buried shrub has a large effect on the modeled SWE. Even layering (points 4 and 5) can cause the SWE and the average density to be slightly over-predicted or under-predicted due to scattering of the sound pressure wave at the snow interfaces.

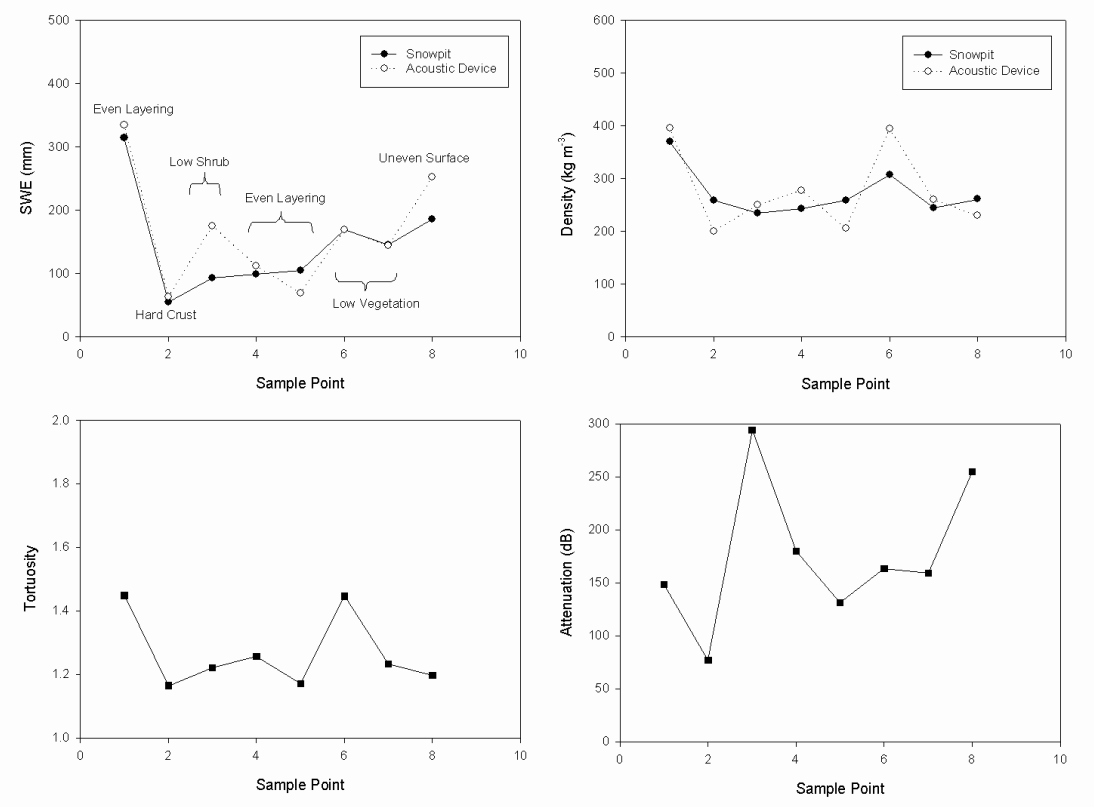

Figure 4. Results for the Granger Basin (GB) site, Yukon Territory

The tortuosity results for GB strongly suggest that tortuosity is highly variable along the transect length. The tortuosity ranges from 1.45 to 1.17, with higher tortuosities observed for points with larger amounts of SWE. The average attenuation of the SPL is 179 dB. Although this attenuation may be unrealistically high, the acoustic calculations of attenuation still suggest that snow is a highly-attenuating material. It is interesting to note that sample point 2 has the lowest attenuation compared to the other points along the transect. It is possible that the hard wind crust observed at this sample point acts as an acoustic lens, focusing the incident beam and reducing scattering.

Because very thick wind crusts and ice layers were observed in snowpack stratigraphy, the Granger Basin site suggests that the acoustic technique can still perform reasonably well for snow that has accumulated in a complex fashion on natural landscapes. It should be noted that dense shrubs precluded use of the ESC30 snow tube in these GB sites – the tube became trapped in the vegetation and disturbed the snowpack.

Table 2. Acoustic model comparisons.

Site	Comparison	R^2	% Difference	RMSE[a] (mm)
Granger Basin GB	Snowpit & Acoustic	0.83	15	41
Boreal Forest BF	Snowpit & ESC30	0.81	14	31
Boreal Forest BF	ESC30 & Acoustic	0.57	26	38
Boreal Forest BF	Snowpit & Acoustic	0.52	12	16
Burstall Pass BP-open	Snowpit & ESC30	0.33	19	77
Burstall Pass BP-open	Snowpit & Acoustic	0.60	6	25
Burstall Pass BP-open	ESC30 & Acoustic	0.38	36	111
Burstall Pass BP-ridge	ESC30 & Acoustic	0.72	10	21
Mount Shark MS	ESC30 & Acoustic	0.79	20	23

[a]Root-Mean Squared Error

The BF site (Figure 5, Table 2) also shows the effects of vegetation on the acoustic SWE technique. Owing to buried logs, small trees, detritus from the forest canopy and hard snow layers, scattering of the sound wave was so pronounced that acoustic estimates of SWE could not be obtained for some points due to the absence of a reflected wave that should have been detected by the prototype device. These missing acoustic data points occurred at positions along the transect where logs were embedded under the snow surface. The acoustic SWE could only be determined in clearings where a smaller amount of buried vegetation was present. Buried twigs and branches were responsible for the variation observed at the other sampling points.

The acoustic densities were increasingly over-predicted beyond the third sample point in the BF transect. Because the acoustic SWE estimates are close to the SWE values determined by gravimetric sampling, there is a corresponding under-prediction of average acoustic snow depth.

This could suggest that at the BF site the procedure of averaging the densities when calculating SWE does not produce more accurate results, and that the geometric shape factor cannot be taken as being a constant value.

The attenuation of the sound wave at the sample points where acoustic SWE was able to be determined was close to 150 dB, and showed little variation over the transect length. Aside from the scattering of the sound wave by buried vegetation, it is possible that other processes could have caused attenuation of the wave. As discussed in Part I (Kinar and Pomeroy, *this issue*), relaxation processes could have interfered with the propagation of sound through the snowpack. There is a need for further research to test the validity of this assumption.

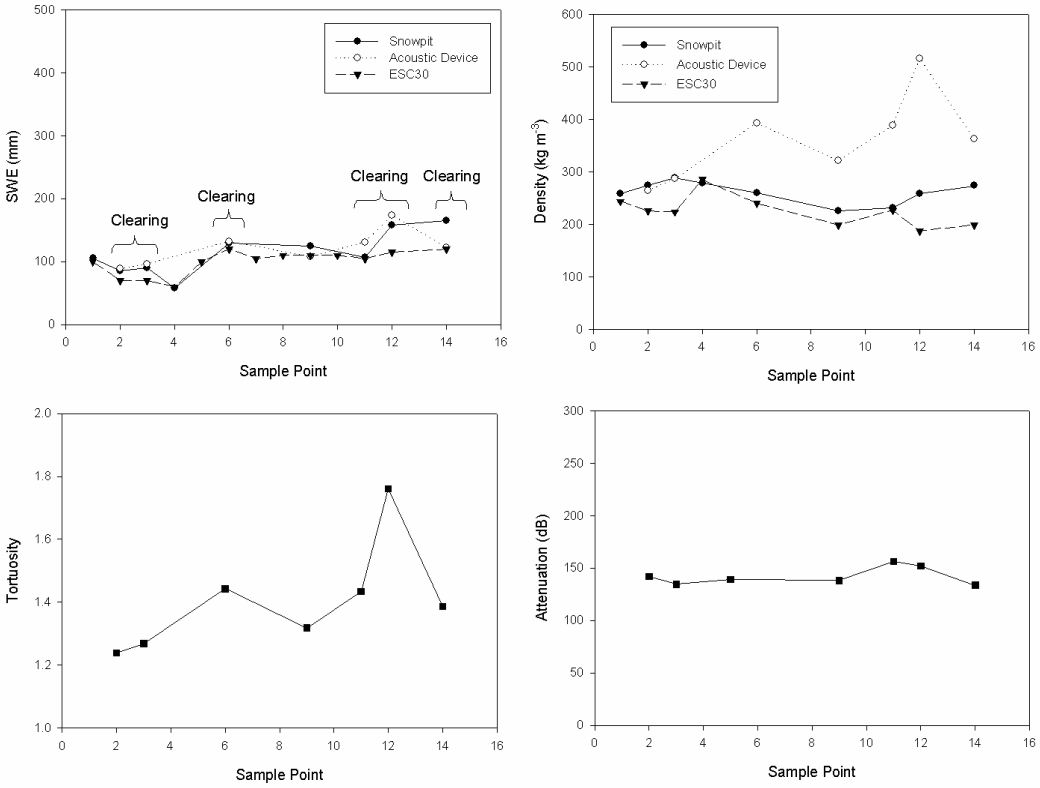

Figure 5. Results for the Boreal Forest (BF) site, Yukon Territory.

Rocky Mountain sites

The data collected at the Burstall pass site (BP-open, Fig. 6, Table 2) demonstrated the effects of wet, melting snow on the acoustic technique. The average difference between the ESC30 and snowpit SWE is 5% higher than the difference in SWE observed between these two types of observations at the boreal forest site (BF) in the Wolf Creek basin and suggests problems with ESC30 measurements under these conditions. The average percentage difference between the snowpit and acoustic measurements of SWE was lower than the percentage differences between these two measurements at the Wolf Creek sites and similar to the differences observed at the BP-ridge site. Although the Biot theory model (Biot, 1956a; Biot, 1956b) cannot be used for wet snow because the pore spaces of the snowpack have a mixture of air and water, and the assumption of this model applied to snow is that the pore spaces are only saturated with air (Johnson, 1982), the results show that the acoustic technique can still produce estimates of SWE that are accurate. Smaller percentage differences occurred between snowpit and acoustic measurements of SWE as compared to ESC30 and snowpit measurements, suggesting superior performance of the acoustic measurement over the snow tube if one assumes that the snowpit is the most reliable observation method. Estimates of density, tortuosity, and attenuation were generally constant over the entire transect length. The acoustic and gravimetric densities were also in good agreement along the transect length.

In contrast, the SWE transect situated on the ridge near the Burstall Pass parking lot (BP-ridge, Figure 7, Table 2) had low differences between the ESC30 and acoustic SWE estimates. Higher SWE estimate differences occurred when samples were taken in close proximity to tree wells. The acoustic snow densities were also over-predicted in close proximity to tree wells. This suggests that scattering due to the irregular snow surface near the tree-well results in the density being over-predicted. Acoustic SWE differences could have been under-predicted (sample point 7) and over-predicted (sample point 6) due to lateral propagation of the sound pressure wave though the side of the tree well formation and into the air surrounding the trunk of the tree. ESC30 density measurements may have had greater error near trees due to clumps of buried unloaded snow which can interfere with collection of a snow core. The tortuosity and attenuation values are generally constant over the entire transect length.

For the Mount Shark survey (MS, Figure 8, Table 2), the percentage difference between the ESC30 and acoustic SWE measurements is greater than the difference between estimates for the transect performed on the ridge near the Burstall pass parking lot (BP-ridge) and greater than the differences between ESC30 and acoustic estimates at the Burstall pass site (BP-open). The percentage difference is comparable to the difference between estimates observed at the Granger Basin site (GB). The Mount Shark survey (MS) is particularly encouraging since the SWE determined by gravimetric sampling with the ESC30 and the acoustic estimates of SWE from the model presented in this paper show a strong correlation along the length of the transect, and consequently, the plots of both observations have a similar form. The under-prediction of SWE is thought to occur due to scattering and attenuation of the sound wave by the hard surface crust layer observed at this site. In a similar fashion to the other sites situated in the Rocky Mountains, the tortuosity and attenuation are generally constant over the entire transect length. Scattering caused by the hard surface crust might have also caused the acoustic density to be under-predicted. The acoustic attenuation is high (average 150 dB) and generally constant along the length of the transect.

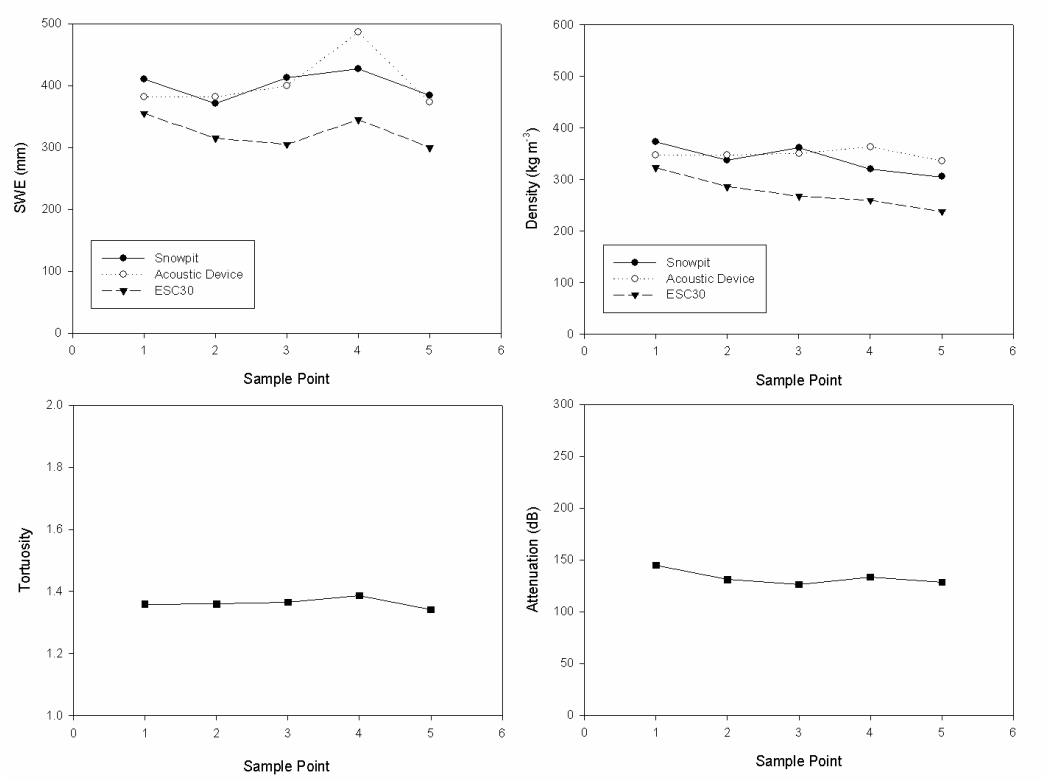

Figure 6. Results for the Burstall Pass (BP-open) site.

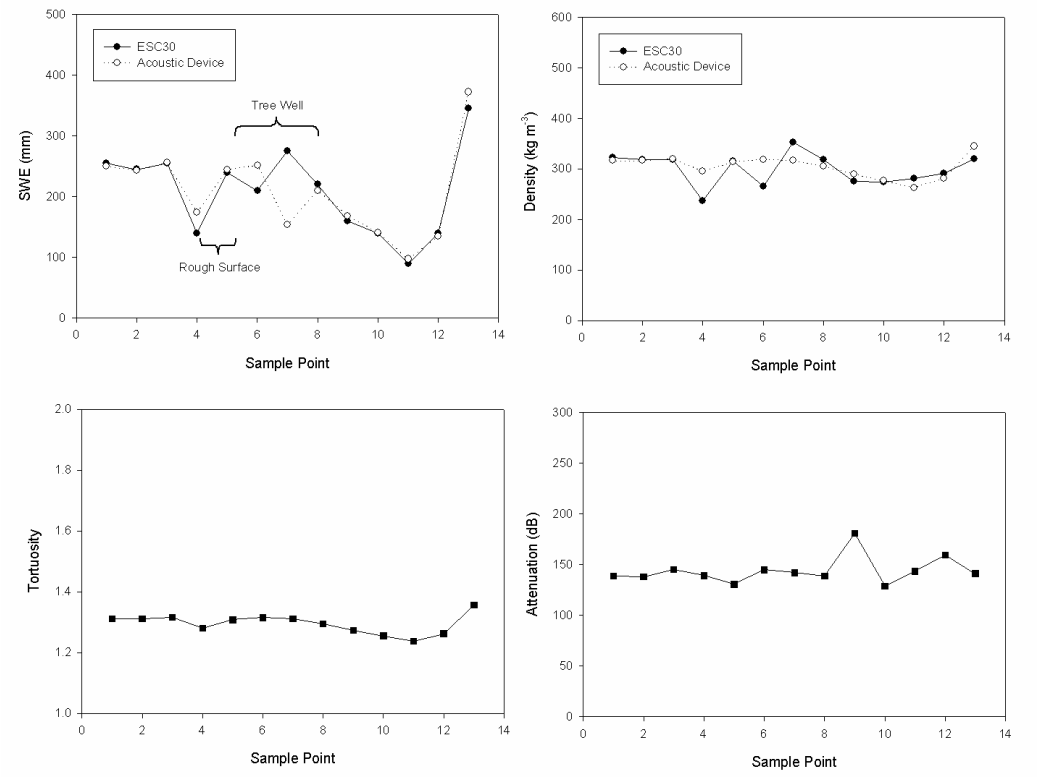

Figure 7. Results for the Burstall Pass (BP-ridge) site.

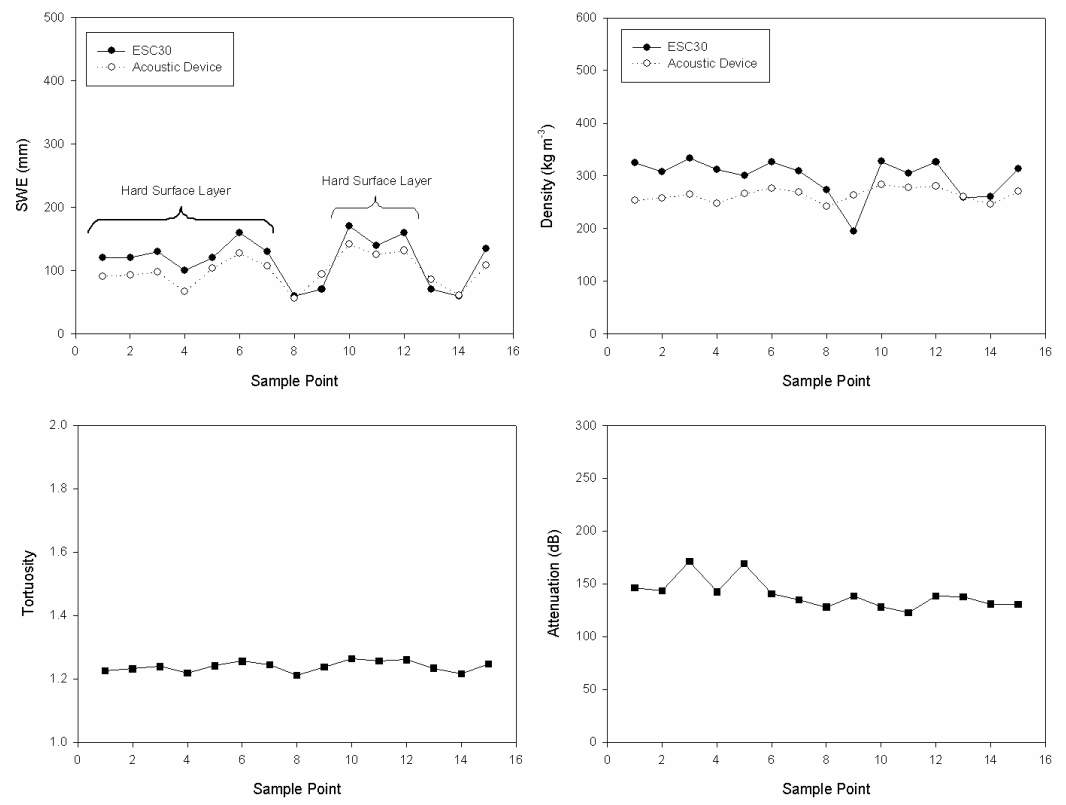

Figure 8. Results for the Mount Shark (MS) site.

SENSITIVITY ANALYSIS

The parameters used for the sensitivity analysis can be divided into two categories: (1) parameters which are sensitive to operator error and the environmental conditions of the sampling location, and (2) parameters which are sensitive to instrumentation error. The parameters chosen for the sensitivity analysis on the variables affected by operator error and sampling locations are: the RMS displacement of the generated fractal interface Δy_{RMS}, the number of harmonic components M, the spatial wave number k, the frequency-scaling parameter b_f used to generate the Weierstrass-Mandelbrot function, the angle of incidence θ_0 of the loudspeaker and the microphone to the snowpack surface, and the density ρ_0 of the air above the air-snow interface. The parameters chosen for the sensitivity analysis on the variables affected by instrumentation error are: the power P of the loudspeaker, the microphone sensitivity L_s, and the aperture angle φ. Figure 9 shows the effect of varying each of these parameters on the model output (calculated SWE). Each parameter was varied while all other parameters were held constant. The sensitivity analysis was conducted using as input all of the collected data at the Yukon and Rocky Mountain sites.

Operator error and sampling location

Varying $\Delta y_{\mathrm{RMS}} \in [0.3, 20.1]$ shows that improper selection of this parameter can cause a maximum reduction in SWE of 200 mm (Figure 9a). The reduction of SWE is on the same order of magnitude of the acoustic SWE values found at each of the sampling points. If $\Delta y_{\mathrm{RMS}} > 20.1$, the change in SWE remains at the threshold value of -200 mm and does not vary.

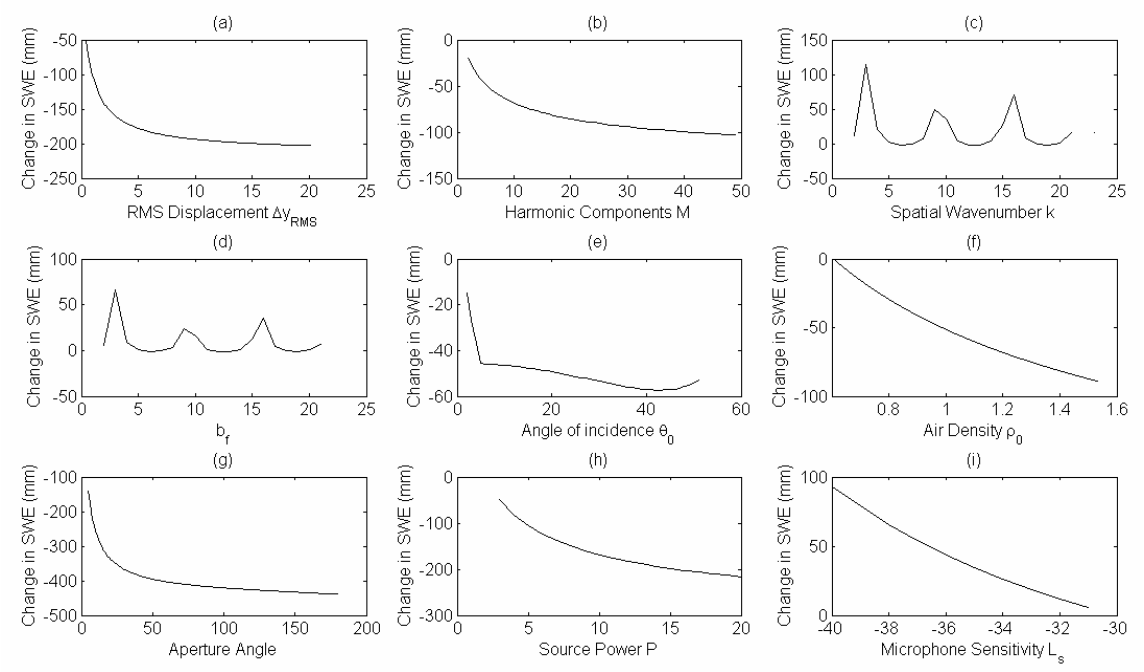

Figure 9. Sensitivity analysis of the acoustic model.

Increasing the number of harmonic components by varying $M \in [1,49]$ shows that improper selection of M can cause a change in the output SWE of up to 100 mm (Figure 9b). In a similar fashion to the Δy_{RMS} parameter, the reduction of SWE is on the same order of magnitude of the acoustic SWE values, and the change in SWE reaches a threshold value of 100 mm change for $M > 49$.

On the intervals $k \in [1,23]$ and $b_f \in [1,21]$, the change in SWE for parameters $\{k, b_f\}$ shows a cyclic relationship (Fig. 9c, Fig. 9d). The maximum change in SWE for these parameters is similar to the change in SWE caused by increasing the number of harmonic components M. Outside of these ranges for $\{k, b_f\}$, the model becomes unstable and it is impossible to calculate SWE.

Compared with changes in the air density ρ_0, the angle of incidence θ_0 is the least sensitive of all parameters (Figure 9e). For angles greater than 5 degrees, the change in SWE abruptly swings to a negative change of approximately 45 mm, and then gradually reaches local minima at around 45 degrees to the normal.

The air density ρ_0 was assumed to be constant at both of the sites ($\rho_0 = 1.292$ kg m^{-3}). The result of the sensitivity analysis (Figure 9f) shows that the SWE can be under-predicted by a maximum of 100 mm over the range of air densities $\rho_0 \in [0.694, 1.51]$. This suggests that changes in air density may have a significant effect on the calculated SWE, and it would be feasible to measure air pressure and relate this to air density when future versions of the acoustic sampling gauge are created.

However, changes in air pressure with elevation and changes in the temperature at different sampling locations will also modify the acoustic power of the loudspeaker and the microphone sensitivity because both of these transducers are mechanical devices. There is also a possibility that changes in air pressure and temperature can modify the effective aperture angle of the loudspeaker. The aperture angle is dependent on the shape of the loudspeaker and the displacement of the moving armature magnetic coil. The spectral power of the signal produced by the loudspeaker will also be affected. Because the sensitivity analysis only changes the numerical inputs to the model, it does not consider these environmental changes which might have compensated for a fixed air density used in this operational version of the model. There is a need

to investigate the environmental effects on the measurement system so that these effects can be either included in the model or characterized as being insignificant.

Instrumentation error

Figure 9e shows that the aperture angle of the loudspeaker is the most sensitive parameter in the model. The change in calculated SWE can be as great as 400 mm for aperture angles approaching 180 degrees. For errors in small aperture angles $\varphi \to 0$, the change in calculated SWE can be as great as the maximum change in the parameters $\{\Delta y_{\mathrm{RMS}}, M, k, b_f\}$. This indicates that precise knowledge of the aperture angle is required so that accurate measurements of acoustic SWE can be obtained.

Improper selection of the source power P of the loudspeaker (Figure 9g) can cause a change in the output SWE that is similar to the calculated change in Δy_{RMS}. However, compared to the change in Δy_{RMS}, the reduction of SWE is more gradual on the interval $P \in [1, 20]$.

Changes in the microphone sensitivity $L_s \in [-40, -30]$ show a gradual increase in calculated SWE (Figure 9i) as the microphone sensitivity is increased (i.e. $L_s = -30$ is less sensitive than $L_s = -40$). Because the maximum change in SWE is similar to a change in $\{M, k\}$, the sensitivity analysis shows that L_s is an important factor to measure when characterizing an acoustic SWE system before deployment.

CONCLUSION

The experiments conducted over two winter field seasons demonstrated that using a modified theory (Kinar and Pomeroy, *this issue*) and a signal processing procedure (Kinar and Pomeroy, 2008), it is possible to determine SWE by an acoustic wave in natural environments characterized by snow with a high liquid water content, wind crusts and vegetation. The modified theory compensated for acoustic scattering by generating a rough fractal snow interface and tracking the footprint of the beam as the sound wave exhibited geometric spreading.

The wide-bandwidth Maximum Length Sequence (MLS) signal sent sound pressure waves of a number of different frequencies into the porous snow medium. Although lower frequency waves will have lessened attenuation rates, the wide-bandwidth MLS signal also helped to ensure that frequencies greater than the threshold frequency $\tilde{\omega}$ propagated through the snowpack. Further research is required to properly identify the effective bandwidth of frequencies that can be used in this acoustic technique. Due to the work of Albert (1993), it is suspected that lower frequencies of sound will be the most effective.

Sensitivity analysis of the parameters in the model shows that changes in the air density ρ_0 has an appreciable effect on the model output. This suggests that air density cannot be always considered as a constant value. Because extreme fluctuations in air density may occur at high elevations in the mountains, the prototype devices could have included barometric sensors or could have prompted the user to enter in an estimate of elevation. Further experimentation is required to assess if this is a necessity on acoustic devices deployed at high elevations.

Although the Biot model of sound propagation assumes that the pore spaces of the porous material are completely air-filed, the results of these experiments demonstrate that similar estimates of SWE are still obtained when the snowpack is wetted. The acoustic results have a higher accuracy when compared to estimates of SWE from snowpit measurements rather than a snow tube because the layered gravimetric sampling allows for a depth-integrated estimate of the density and is therefore a more accurate estimator of SWE than the bulk estimate from the ESC30 tube. Further research is required to develop a model that is able to incorporate the effects of snowpack wetness in the equations used to determine SWE. Testing of this new model would require quantitative estimates of snow wetness, which can be obtained by dielectric and capacitance observations.

Further research is also required to mathematically model the interactions of the sound wave with ice layers and vegetation. Prediction of sound wave scattering by buried vegetation may help to provide insights into mitigating this effect and improving the acoustic estimates of SWE.

Additional mathematical modeling may help to identify the possible acoustic focusing effects of ice layers and wind crusts that may function in a similar fashion to acoustic lenses.

ACKNOWLEDGMENTS

We would like to acknowledge Warren Helgason and Pablo Dornes (University of Saskatchewan), Rick Janowicz (Yukon Environment), Anne Sabourin (L'Ecole Polytechnique Paris, France), and Richard Essery (University of Edinburgh, Scotland) for assistance with field work. The hospitality of the University of Calgary Biogeoscience Institute is recognized. Funding was provided by NSERC, the International Polar Year (IPY), and CFCAS through the IP3 Network.

REFERENCES

Albert DG. 1993. *Attenuation of outdoor sound propagation levels by a snow cover, CRREL Report 93-20*. Cold Regions Research and Engineering Laboratory: Hanover, New Hampshire.

Biot MA. 1956a. Theory of propagation of elastic waves in a fluid-saturated porous solid I. Low Frequency Range. *Journal of the Acoustical Society of America* **28**(2): 168-178.

Biot MA. 1956b. Theory of propagation of elastic waves in a fluid-saturated porous solid. II. Higher frequency range. *Journal of the Acoustical Society of America* **28**(2): 179-191.

Borish J, Angell JB. 1983. An efficient algorithm for measuring the impulse response using pseudorandom noise. *Journal of the Audio Engineering Society* **31**(7): 478-487.

Granger RJ. 1999. Partitioning of energy during the snow-free season at the Wolf Creek Research Basin. In *Wolf Creek Research Basin: Hydrology, Ecology, Environment, Proceedings of a Workshop held in Whitehorse, Yukon, 5-7 March 1998,* Pomeroy JW, and Granger, R.J. (ed). National Water Research Institute: Saskatoon, Saskatchewan.

Johnson JB. 1982. On the application of Biot's theory to acoustic wave propagation in snow. *Cold Regions Science and Technology* **6**: 49-60.

Kinar NJ, Pomeroy JW. 2007. Determining snow water equivalent by acoustic sounding. *Hydrological Processes* **21**: 2623-2640.

Kinar NJ, Pomeroy JW. 2008. Automated determination of Snow Water Equivalent by acoustic reflectometry. *IEEE Journal of Geoscience and Remote Sensing*: submitted.

Kinsler LE, Frey AR. 1962. *Fundamentals of Acoustics, 2nd Edition*. John Wiley & Sons: New York.

Moore HM, Attenborough K, Rogers J, Lee S. 1991. In-situ acoustical investigations of deep snow. *Applied Acoustics* **33**(4): 281-301.

Raichel DR. 2006. *The Science and Applications of Acoustics, 2nd Edition*. Springer Science+Business Media, LLC: New York.

Rife DD, Vanderkooy J. 1989. Transfer-function measurement with maximum-length sequences. *Journal of the Audio Engineering Society* **37**(6): 419-444.